

Eigenvalue Analysis of Peroxisome Proliferator-Activated Receptor γ Agonists

Chenzhong Liao,^{†,‡} Aihua Xie,^{†,‡} Leming Shi,[†] Jiaju Zhou,[‡] and Xianping Lu^{*,†}

Chipscreen Biosciences, Ltd., Research Institute of Tsinghua University, Suite C301, P.O. Box 28, Shenzhen, Guangdong 518057, China, and Institute of Process Engineering, Chinese Academy of Sciences, P.O. Box 353, Beijing 100080, China

Received May 30, 2003

Eigenvalue analysis (EVA) was conducted on a series of potent agonists of peroxisome proliferator-activated receptor γ (PPAR γ). Predictive EVA quantitative structure–activity relationship (QSAR) models were established using the SYBYL package, which had conventional r^2 and cross-validated coefficient (q^2) values up to 0.920 and 0.587 for the AM1 method and 0.863 and 0.586 for the PM3 method, respectively. These models were validated by a test set containing 18 compounds. The capability to predict by these two models for PPAR γ agonists, with the best predictive r^2_{pred} value of 0.614 for AM1 and 0.822 for PM3 methods, set a successful example for applying a similar approach in building QSAR models for PPAR α and δ that could potentially offer a new opportunity in the design of novel PPAR modulators.

INTRODUCTION

Peroxisome proliferator-activated receptors (PPARs) belong to the nuclear receptor superfamily of ligand-activated transcription factors. There are three known subtypes, namely, the PPAR α , PPAR γ , and PPAR δ distributed in a spatial fashion among different tissues. PPARs form heterodimers with retinoid X receptor (RXR) and activate subsets of genes controlling lipids, carbohydrate, and energy homeostasis.¹ Thus, inappropriate activation or inactivation of PPARs directly linked to pathological processes such as type 2 diabetes, cardiovascular diseases, obesity, and dyslipidemia.

Recently, a class of compounds termed thiazolidinedione (TZD) has been developed as treatment for type 2 diabetes to reduce hyperglycemia by promoting insulin action. Their effects are proposed to result from initiation and modulation of adipocyte differentiation by agonist activity of PPAR γ . Although TZD type treatments improve insulin resistance, they offer little protection from eminent cardiovascular risk associated with type 2 diabetes. Side effects such as obesity, edema, and anemia in treated patients further hamper their extended use in the management of the diseases. It has been reported that PPAR α stimulates peroxisomal proliferation that enhances fatty acid oxidation, leading to reduced fatty acids level in blood.² Most recently, PPAR δ was reported to be a key modulator for fat burning.³ Therefore, development of new treatments that have insulin sensitizing and cholesterol/triglycerides-lowering effects are of general interest.

Three-dimensional quantitative structure–activity relationship (3D QSAR) methods can be used as powerful tools for discovering new compounds with higher bioactivity. The structures of the PPAR γ LBD (ligand-binding domain) that contain different agonists have been determined by X-ray

crystallography.^{4–6} A series of tyrosine-based PPAR γ agonists,^{7–9} exemplified by GI 262570, and other structurally diverse PPAR γ agonists have been developed.^{10–14} Therefore, those data can be used as a training set to build proper QSAR models in an attempt to develop a methodology to better and quicker design of PPAR ligands. Kurogi had developed a 3D QSAR model for antidiabetic TZDs using the Apex method to identify molecular features.¹⁵ However, this model is insufficient to explain more complex compounds such as tyrosine-based PPAR γ agonists due to the inclusion of only seven compounds of selected TZD in the training set.

CoMFA¹⁶ (comparative molecular field analysis) and CoMSIA^{17–19} (comparative molecular similarity indices analysis) are well-known 3D QSAR techniques with abilities to visualize and interpret the obtained correlations in terms of field contributions. However, both methods require superimposing of all the molecular structures in the training set. Unlike CoMFA and CoMSIA, eigenvalue analysis (EVA) provides a conformationally sensitive but superposition-free descriptor that has been shown to perform well with a wide range of data sets and biological end points.^{20–24}

In this paper, we performed the data analysis using EVA and established relevant QSAR model with good predication of new structural requirements of a set of PPAR γ agonists.

METHODS

EVA Descriptors. EVA is derived from calculated infrared-range (IR-range) vibrational frequencies. The normal modes of vibration for an input molecule that was energy-minimized accordingly are calculated using a classical normal coordinate analysis (NCA), normally included in MOPAC or some other molecular mechanics packages. The eigenvalues taken from such an analysis provide normal-mode frequencies from which the EVA descriptor is derived. A nonlinear structure will have an eigenvalue of $3N - 6$, while a linear structure, for example carbon dioxide, will have an eigenvalue of $3N - 5$, where the N is the number of atoms in a molecule. The normal modes of vibration are used to

* Corresponding author phone: +86-755-26711889; Fax: +86-755-26957291; e-mail: xplu@chipscreen.com.

[†] Research Institute of Tsinghua University.

[‡] Chinese Academy of Sciences.

construct a vibrational profile between 0 and 4000 cm^{-1} by summing (convoluting) a series of Gaussian distributions, with one centered on each normal mode f_i . A Gaussian kernel of fixed standard deviation σ (cm^{-1}) is then placed over each eigenvalue; this results in $3N - 6$ (or $3N - 5$) overlapping kernels.

EVA vectors are then built by sampling this artificial vibrational profile at intervals across this profile. The distance between sampled frequencies (δ) is also an important EVA parameter. A smaller value of δ is generally desirable. Default values for σ and δ have previously been set at 10 and 5 cm^{-1} , respectively,²⁰ which provide a descriptor consisting of 800 (i.e., 4000/5) variables. Normally, the range chosen for EVA encompasses the frequencies of all fundamental molecular vibrations. EVA descriptors are somewhat dependent on the conformation used in their calculation, particularly when the frequency is below 1000 cm^{-1} . The frequencies lower than 200 cm^{-1} do not contribute to the model significantly, and most of the calculations therefore were done with a range of 200–4000 cm^{-1} . For the purpose of this study, AM1 and PM3 Hamiltonians have been used to calculate normal modes of vibration for an input structure.^{25,26}

All molecular modeling techniques and EVA studies described here were performed using SYBYL²⁷ version 6.81 running on a Silicon Graphics O2+ (R12000) workstation with the IRIX 6.5 operating system.

Data Set. The structures of 97 agonists including 6 TZDs and 91 tyrosine-based compounds and their binding affinities (pK_i) to PPAR γ used in this study were extracted from publications originated from the same laboratory.^{7–9} All compounds have been shown to be potent agonists of PPAR γ .

A training set of 79 PPAR γ agonists was used for EVA analyses. These compounds are summarized in Table 1. Because only the (*S*)-enantiomers of the TZDs and tyrosine-based compounds bind to the receptor with high affinity,²⁸ the pK_i values of the racemates are augmented with log 2, i.e., 0.30 in order to eliminate the error. And the structures of the racemates used in the modeling are treated as *S* conformation.

Molecular Conformation. Except TZDs, all the tyrosine-based compounds have high flexibility. Albeit EVA might be described as a “2 $\frac{1}{2}$ D” descriptor,²⁹ EVA descriptors are somewhat dependent on the conformation used in the calculation, particularly when the frequency is below 1000 cm^{-1} . To calculate EVA values, we assume the conformations constructed here are similar to those reported in PPAR γ LBD crystal structures from Brookhaven Protein Data Bank (PDB).³⁰ In this study, 1FM6⁴ and 1FM9³¹ were used as the references. 1FM6 contains a TZD, rosiglitazone (**5**), and 1FM9 contains a tyrosine-based compound, farglitazar (**15**). To obtain the likely conformation, we adopted a systematic search that met specific distance constraints according to the active conformations of **5** and **15** in the 1FM6 and 1FM9 crystals. The low-energy conformations of these compounds obtained were minimized using the TRIPOS force field³² and subsequently used in the analysis. When applying the AM1 Hamiltonian, partial atomic charges were calculated using the semiempirical program MOPAC 6.81.³³

Partial-Least-Squares Analysis. The EVA descriptors were used as independent variables, and pK_i values were used

as dependent variables in partial-least-squares (PLS) regression analyses to derive 3D QSAR models using the standard implementation in the SYBYL package. The predictive value of the models was evaluated first by leave-one-out (LOO) cross-validation. The optimal number of components was determined by selecting the smallest S_{PRESS} value that corresponds to the highest cross-validated coefficient q^2 value. The same number of components was subsequently used to derive the final QSAR models. In addition to the q^2 , the corresponding S_{PRESS} , the number of components, the conventional correlation coefficient r^2 , and its standard error S were also computed.

RESULTS AND DISCUSSION

EVA QSAR Models. When performing the EVA analysis according to the default values ($\sigma = 10 \text{ cm}^{-1}$; $\delta = 5 \text{ cm}^{-1}$; AM1), and the training set containing 79 compounds, the result was not satisfactory since the cross-validated coefficient q^2 was only 0.285 (see Table 2, where the q^2 , S_{PRESS} , r^2 , F , and S values were computed as defined in SYBYL). $\text{Pr}^2 = 0$ means the probability of obtaining the observed F -ratio value by chance alone, if the target and the explanatory variables themselves are truly uncorrelated. When $\text{Pr}^2 = 0$ is zero, the results are not by chance and are significant. The training set was then screened for outliers. Theoretically, agonists with residuals between experimental and predicted pK_i above or equal to 4*S* were considered outliers; empirically, agonists with a residual above 1.0 were considered outliers. In this study, however, agonists with residuals between experimental and predicted pK_i values above 1.5 logarithm units were considered outliers to derive good predictive QSAR models. In the first EVA analysis with the default parameters, because compounds **6**, **29**, **66**, and **67** have residuals of +1.97, −1.68, −2.09, and −1.79 logarithm units, respectively, they were selected as outliers. There are several reasons that may account for the outliers, for example, an incorrectly measured experimental value, a different binding conformation, a significant difference in the physicochemical properties, or structural uniqueness. Compound **6** appears to have higher activity than expected when compared to compounds **7–9**; compound **29** appears to have lower activity than expected when compared to compounds **30** and **15**; and compounds **66** and **67** appear to have lower activity than expected when compared to compounds **63–65** and **68**. It is possible that experimental errors are introduced when the bioactivities of these compounds were measured. When dropping them from the training set, we reperfomed the EVA analyses. The results are also shown in Table 2. It shows the models based on 75 compounds are indeed improved over the model based on 79 compounds. Thus, all the following EVA analyses were constructed on the 75-compound data set, and all the subsequent results and discussion are based on the 75-compound models.

A systematic evaluation was made of the quality of EVA QSAR models based upon descriptors derived using a wide range of σ values. Descriptors were derived using all values of σ in the set {1, 2, 3, 4, 5, 8, 10, 15, 20, 25, 35, and 50}. The results of EVA analyses using AM1 and PM3 methods are summarized in Table 3 and Table 4, respectively. When using the AM1 method, $\sigma = 3 \text{ cm}^{-1}$, $\delta = 5 \text{ cm}^{-1}$ yielded

Table 1. Structure of 79 Agonists in the Training Set and Their Actual Activities

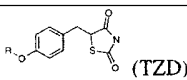
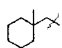
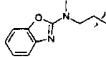
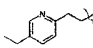
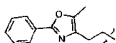
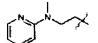
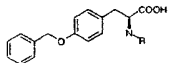
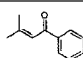
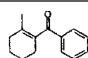
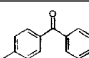
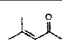
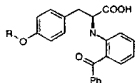
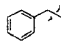
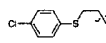
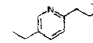
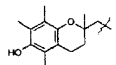
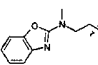
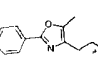
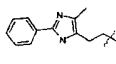
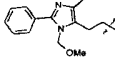
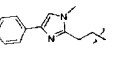
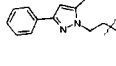
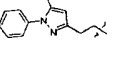
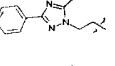
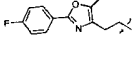
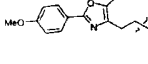
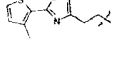
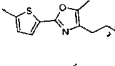
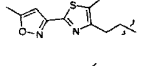
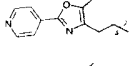
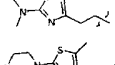
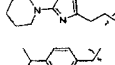
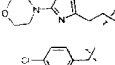
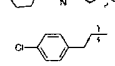
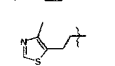


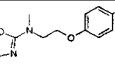
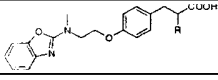
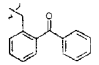
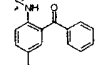
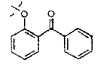
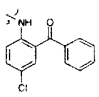
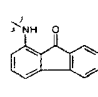
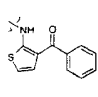
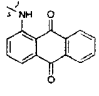
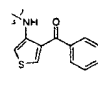
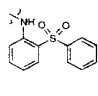
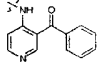
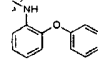
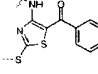
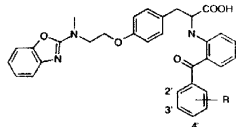
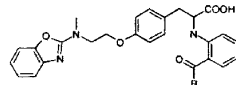
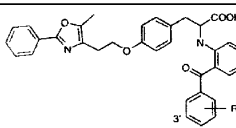
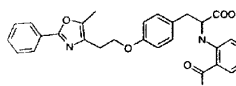
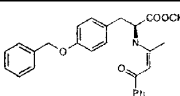
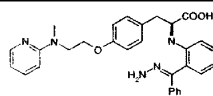
<div> (TZD)</div>								
no.	R	pK _i	no.	R	pK _i	no.	R	pK _i
1		5.81	2		7.87	3		6.21
4		8.67	5		7.63			
<div></div>								
no.	R	pK _i	no.	R	pK _i	no.	R	pK _i
6		7.93	7		6.10	8		5.90
9		5.71						
<div></div>								
no.	R	pK _i	no.	R	pK _i	no.	R	pK _i
10		6.79	11		7.94	12		8.19
13		8.28	14		8.83	15		8.94
16		8.59	17		8.70	18		9.16
19		8.75	20		8.90	21		8.32
22		8.80	23		8.96	24		8.72
25		9.07	26		9.05	27		8.85
28		7.56	29		6.77	30		9.11
31		8.36	32		6.98	33		7.41
34		8.03	35		7.73			
<div></div>								
no.	R	pK _i	no.	R	pK _i	no.	R	pK _i
36		7.55	37		8.17	38		7.49
39		8.36	40		7.07	41		7.93
42		8.29	43		8.89	44		6.91
45		7.11	46		8.43	47		7.67

Table 1 (Continued)

								
no.	R	pK _i	no.	R	pK _i	no.	R	pK _i
48	2'-CF ₃	8.87	49	3'-CF ₃	8.88	50	4'-CF ₃	8.59
51	2'-CH ₃	8.95	52	4'-CH ₃	8.85	53	2'-OCH ₃	9.06
54	3'-OCH ₃	8.94	55	3'-OCH ₂ Ph	7.57	56	4'-Ph	7.61
								
no.	R	pK _i	no.	R	pK _i	no.	R	pK _i
57	cyclopentyl	8.49	58	cyclohexyl	8.39	59 ^a	cyclohexyl	5.81
60	cycloheptyl	7.70	61	3-thienyl	8.93	62	1-naphthyl	8.79
								
no.	R	pK _i	no.	R	pK _i	no.	R	pK _i
63	4'-CH ₂ OH	8.68	64	4'-CH ₂ NMe ₂	8.11	65	3'-CH ₂ OH	8.77
66	3'-COOH	6.39	67	3'-CH ₂ NMe ₂	6.24	68	3'-NH ₂	8.79
								
no.	R	pK _i	no.	R	pK _i	no.	R	pK _i
69	cyclohexyl	8.79	70 ^a	cyclohexyl	6.72	71	3-pyridyl	9.03
72	4-pyridyl	8.74	73	NHMe	8.11	74	NMe ₂	6.90
75	OMe	8.43	76	OEt	8.52	77	OiPr	9.01
Other								
no.	Structure	pK _i	no.	Structure	pK _i			
78		6.12	79		6.79			

^a This compound is a (*R*)-enantiomer.

the best correlation with $q^2 = 0.587$ by means of three principal components. The conventional r^2 for this analysis was 0.920. When using the PM3 method, $\sigma = 20 \text{ cm}^{-1}$, $\delta = 5 \text{ cm}^{-1}$ yielded the best correlation with $q^2 = 0.586$ by means of five principal components. The conventional r^2 for this analysis was 0.863. The plots of predicted versus actual

binding affinities for the fitted PLS analyses are shown in Figure 1a corresponding to the results of the AM1 method, $\sigma = 3 \text{ cm}^{-1}$, $\delta = 5 \text{ cm}^{-1}$, and Figure 1b corresponding to the results of the PM3 method, $\sigma = 20 \text{ cm}^{-1}$, $\delta = 5 \text{ cm}^{-1}$.

It was noted that the model was not improved upon increasing the resolution factor (σ) to 5 and 10 cm^{-1} when

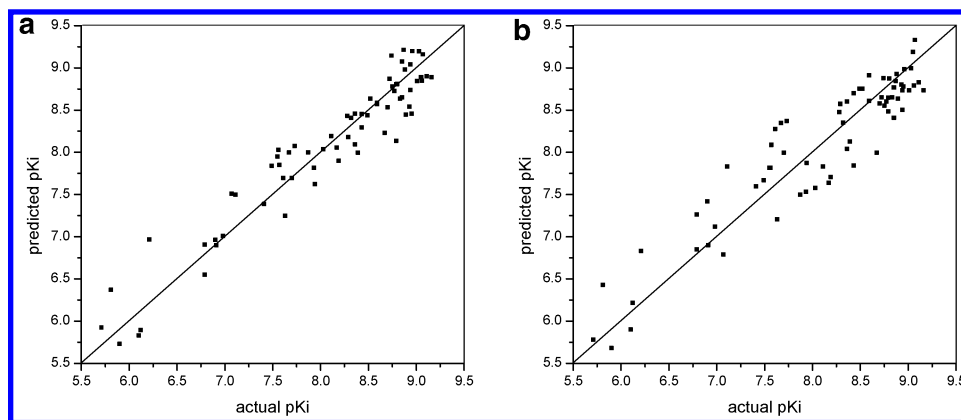


Figure 1. Fitted predictions versus actual binding affinities for the 75 agonists of the training set (four outliers were picked out). The predicted values were obtained by PLS analyses using the AM1 (a) and PM3 (b) method: in a, $\sigma = 3 \text{ cm}^{-1}$, $\delta = 5 \text{ cm}^{-1}$; in b, $\sigma = 20 \text{ cm}^{-1}$, $\delta = 5 \text{ cm}^{-1}$.

Table 2. PLS Statistics of EVA Models When Using Default Parameters ($\sigma = 10 \text{ cm}^{-1}$; $\delta = 5 \text{ cm}^{-1}$; AM1)

PLS statistics	79-compd model	75-compd model
q^2	0.285	0.529
PLS components	2	3
S_{PRESS}	0.678	0.692
r^2	0.626	0.779
S	0.508	0.482
F	48.11	62.24
norm coeff	5.984	3.290
Pr^2	0	0
r^2_{pred}	0.529	0.566

the AM1 method was used. If σ increased more, the q^2 declined slightly; however, it increased again after $\sigma = 35 \text{ cm}^{-1}$ (see Figure 2). In contrast, the trend for q^2 using the PM3 method, is different from the one by using the AM1 method. q^2 at first climbed quickly and reached a maximum value at $\sigma = 20 \text{ cm}^{-1}$, and then it declined as revealed from Figure 2.

Predictive Power of the Analyses. To test the predictive power of the EVA models, 18 additional agonists (including 1 TZD and 17 tyrosine-based compounds; see Table 5) were selected as a test set. The conformations of these molecules

were obtained by the same protocol as that already described for the agonists of the training set used. The plots of predicted versus actual binding affinity for the test set molecules are shown in Figure 3, in which the values correspond to the models derived from the AM1 method where $\sigma = 3 \text{ cm}^{-1}$, $\delta = 5 \text{ cm}^{-1}$ and the PM3 method where $\sigma = 20 \text{ cm}^{-1}$, $\delta = 5 \text{ cm}^{-1}$, respectively. In the former model, only one residual was greater than 1 (1.05, compound 85), while, in the later model, the greatest residual was -0.89 (compound 80).

The predictive r^2 (r^2_{pred}) of all EVA models are showed in Table 3 and Table 4. It is interesting to note that all of the r^2_{pred} from the PM3 method are always greater than the one from the AM1 method with regard to the value of q^2 from either method, as shown in Figure 4.

From the above results, it appears that the EVA models built here provided the successful prediction of binding affinities toward PPAR γ .

Comparison of EVA with CoMFA and CoMSIA. We have performed the CoMFA and CoMSIA on the same training set and test set.³⁴ In CoMFA, the best $q^2 = 0.642$, $r^2 = 0.974$, and $F = 288.2$, while, in CoMSIA, the best $q^2 = 0.686$, $r^2 = 0.979$, and $F = 358.2$. Although CoMFA and CoMSIA outperformed EVA in this study, the EVA model

Table 3. Summary of EVA Results Using the 200–4000 cm^{-1} Frequency Range ($\delta = 5 \text{ cm}^{-1}$, AM1)

	$\sigma = 1$	$\sigma = 2$	$\sigma = 3$	$\sigma = 4$	$\sigma = 5$	$\sigma = 8$	$\sigma = 10$	$\sigma = 15$	$\sigma = 20$	$\sigma = 25$	$\sigma = 35$	$\sigma = 50$
q^2	0.458	0.562	0.587	0.572	0.557	0.554	0.528	0.510	0.496	0.484	0.461	0.489
compd	2	3	3	3	2	3	3	3	5	3	5	4
S_{PRESS}	0.730	0.670	0.652	0.662	0.668	0.689	0.692	0.704	0.726	0.721	0.748	0.723
S	0.423	0.268	0.308	0.347	0.433	0.454	0.483	0.517	0.448	0.535	0.526	0.575
r^2	0.830	0.942	0.920	0.899	0.820	0.806	0.776	0.738	0.818	0.708	0.738	0.676
F	126.8	244.77	179.82	136.92	120.15	71.48	61.35	50.20	44.69	45.56	31.14	29.13
Pr^2	0	0	0	0	0	0	0	0	0	0	0	0
norm coeff	3.685	4.478	4.135	3.922	3.353	3.430	3.288	3.243	4.775	3.685	4.664	4.461
r^2_{pred}	0.438	0.554	0.614	0.613	0.603	0.595	0.566	0.543	0.511	0.480	0.508	0.411

Table 4. Summary of EVA Results Using the 200–4000 cm^{-1} Frequency Range ($\delta = 5 \text{ cm}^{-1}$, PM3)

	$\sigma = 1$	$\sigma = 2$	$\sigma = 3$	$\sigma = 4$	$\sigma = 5$	$\sigma = 8$	$\sigma = 10$	$\sigma = 15$	$\sigma = 20$	$\sigma = 25$	$\sigma = 35$	$\sigma = 50$
q^2	0.324	0.451	0.495	0.506	0.541	0.513	0.541	0.555	0.586	0.567	0.534	0.480
compd	4	3	4	4	4	3	4	4	5	6	6	7
S_{PRESS}	0.823	0.744	0.719	0.713	0.689	0.702	0.691	0.676	0.663	0.683	0.705	0.749
S	0.148	0.297	0.251	0.297	0.310	0.425	0.397	0.426	0.387	0.404	0.455	0.481
r^2	0.976	0.925	0.943	0.935	0.917	0.833	0.861	0.835	0.863	0.851	0.816	0.794
F	620.77	192.23	212.37	145.99	133.24	84.49	74.92	63.06	64.05	48.32	37.05	28.84
Pr^2	0	0	0	0	0	0	0	0	0	0	0	0
norm coeff	6.055	4.738	4.924	4.472	4.390	3.668	3.987	4.068	5.189	5.669	5.979	8.255
r^2_{pred}	0.442	0.700	0.773	0.788	0.750	0.772	0.822	0.783	0.675	0.629	0.562	0.561

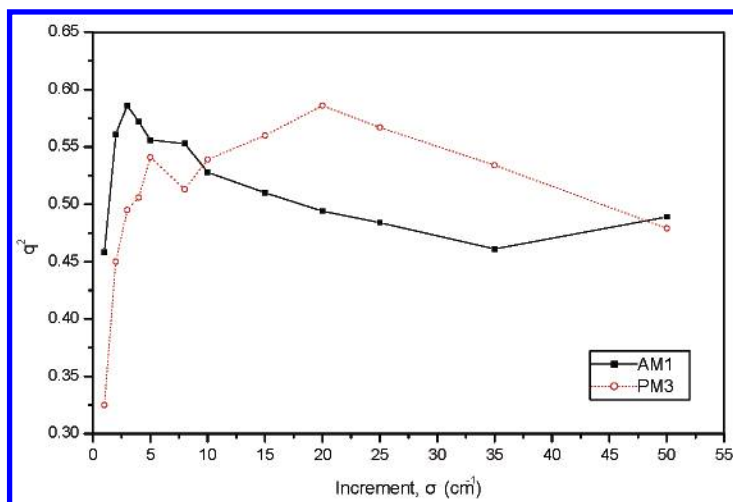


Figure 2. Plots of the variation of q^2 scores with σ . The solid line represents the trend of q^2 when using the AM1 method; the dotted line represents the trend of q^2 when using PM3 method.

Table 5. Structure of 18 Agonists in the Test Set and Their Actual Activities

no.	Structure	pK _i	no.	Structure	pK _i
80		6.82	81		7.29
82		8.62	83		5.88
84		6.98	85		8.85
86		7.48	87		8.48
88		8.96	89		9.06
90		7.71	91		8.87
92		8.55	93		7.48
94		8.86	95		8.31
96		6.49	97		8.11

is still good for predicting the biological binding ability of the new structure toward PPAR γ .

Graphical Interpretation of the Results. Unlike CoMFA and CoMSIA, EVA has no 3D isocontour plots to visualize

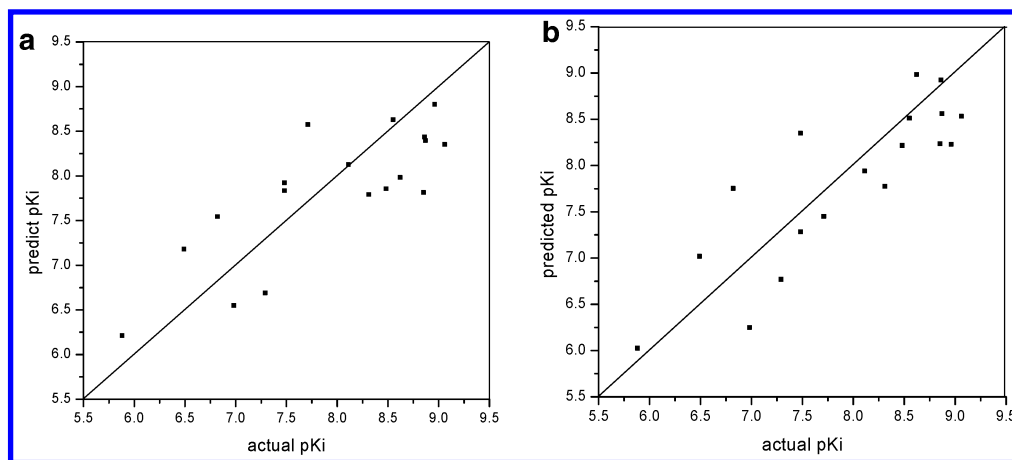


Figure 3. Predicted versus actual binding affinities for the 18 agonists not included in the training set. The predicted values were obtained by PLS analyses using the AM1 method with $\sigma = 3 \text{ cm}^{-1}$, $\delta = 5 \text{ cm}^{-1}$ (a) and the PM1 method with $\sigma = 20 \text{ cm}^{-1}$, $\delta = 5 \text{ cm}^{-1}$ (b).

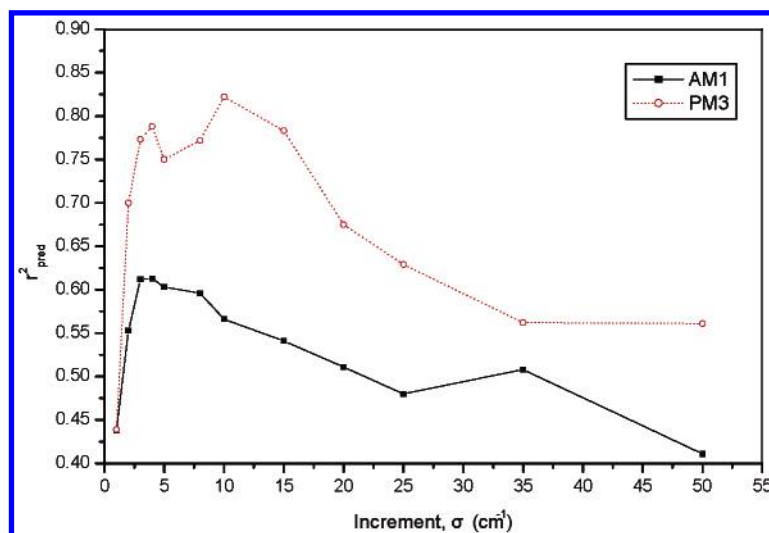


Figure 4. Comparison of the r^2_{pred} gotten by AM1 and PM3 methods. The solid line represents the trend of r^2_{pred} when using the AM1 method; the dotted line represents the trend of r^2_{pred} when using the PM3 method.

those regions of space indicated in the PLS model to reflect positive or negative correlation with biological activity. In fact, the EVA QSAR model uses 2D plots to facilitate interpretation of the observation in a fashion similar to that used to interpret an experimental IR spectrum. In EVA, results are presented as a profile across frequencies ranging from the minimum to the maximum specified for each EVA column when it was created.

As with real infrared spectroscopy, EVA profiles of a compound are also divided into two parts: the fingerprint region ($1\text{--}1500 \text{ cm}^{-1}$) and the functional group region ($1500\text{--}4000 \text{ cm}^{-1}$). The fingerprint region contains a great deal of vibrational information, but most of the group frequencies overlap and are nonspecific. Hence, it is difficult to correlate them with the activity. In contrast, the functional group region contains considerably less information, but it is specific and can be correlated with the activity regarding the presence or absence of particular functional groups. The EVA profiles of compound **1** (ciglitazone, less active) and compound **15** (farglitazar, more active) are shown as the examples in Figure 5 (AM1 method, $\sigma = 10 \text{ cm}^{-1}$, $\delta = 5 \text{ cm}^{-1}$). Vertical axes in the figure represent actual values for

most profiles and run 0 to $5/\sigma$. Color coding is used only to help visualize differences in height across the profiles. The middle line graph (StDev*Coeff) shows the value of this statistic across the range of frequencies included in the descriptor. Some frequencies were dropped from the analysis because they did not vary across the data set (about 300 of 761 frequencies, in this case). Values at such frequencies are set to 0 or simply omitted when graphing, as they are at the right most end of the StDev*Coeff profile. Note that important frequencies show up as dispersion signals—positive peaks preceded or followed (or both) by negative troughs. This pattern follows naturally from the spectral convolution and sampling technique used to create the EVA profiles.³⁵

As shown in Figure 5 concerning the functional group region (at the right part of the profiles, about 3200 cm^{-1}), there are prominent peaks in the hydrogen bond stretching frequency region for the tyrosine-based compounds, for example, compound **15**, that possess two hydrogen bond donor groups, i.e., the OH group at the carboxyl and the NH group at *N*-(2-benzoylphenyl). But for compound **1**, a TZD for example, the peak of the hydrogen bond donor is attenuated because there is only one hydrogen bond donor. And the acidity of the TZD is weaker than carboxylic acid. It has been documented that the more acidic the common

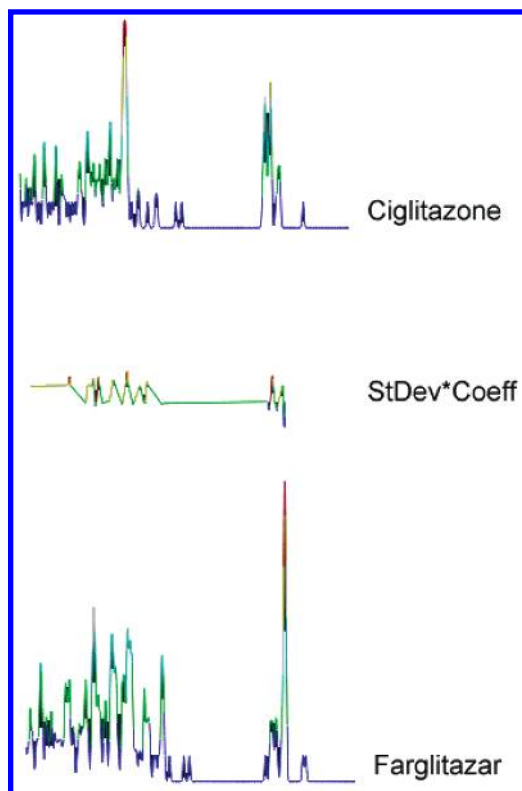


Figure 5. EVA profiles of compounds **1** (ciglitazone) and **15** (farglitazar).

acidic proton is, the more the compound does in activation of the PPAR γ . It is clear that the acidity of tyrosine is stronger than that of TZD. And the other hydrogen bond donor, NH, can form a hydrogen bond with the oxygen atom in *N*-(2-benzoylphenyl). In addition, the larger, more lipophilic moiety, *N*-(2-benzoylphenyl), probably accounts for the greater PPAR γ affinity because it interacts with an area of the ligand-binding domain of PPAR γ that is not accessible to the TZD.³³

CONCLUSIONS

In this paper, the EVA method has been applied successfully to rationalize the PPAR γ agonists of 79 compounds composed of 5 TZDs and 74 tyrosine-based compounds. The EVA QSAR models, which have been achieved without the need to align the structures concerned, have statistical significance and good predictive abilities. The present study has shown that EVA can be used to develop good predictive QSAR models for a structurally diverse data set of compounds.

Through the present results exemplified here, we can apply a similar approach to build other QSAR models for PPAR α and δ . Utilization of those models will likely provide more effective means in designing novel antidiabetic compounds with improved profiles.

ACKNOWLEDGMENT

The authors gratefully acknowledge financial support from the national "863" project of the People's Republic of China and the project of "Most Important Biopharmaceutical Projects" by the Guangdong Province government in China. The authors also want to give special thanks to Drs. Zhibin

Li, Zhiqiang Ning, and Weiming Hu for their support of this project.

REFERENCES AND NOTES

- (1) Willson, T. M.; Brown, P. J.; Sternbach, D. D.; Henke, B. R. The PPARs: From Orphan Receptors to Drug Discovery. *J. Med. Chem.* **2000**, *43*, 527–550.
- (2) Issemann, I.; Green, S. Activation of a Member of the Steroid Hormone Receptor Superfamily by Peroxisome Proliferators. *Nature* **1990**, *347*, 645–650.
- (3) Wang, Y. X.; Lee, C. H.; Tiep, S.; Yu, R. T.; Ham, J.; et al. Peroxisome-Proliferator-Activated Receptor δ Activates Fat Metabolism to Prevent Obesity. *Cell* **2003**, *113*, 159–170.
- (4) Nolte, R. T.; Wisely, G. B.; Westin, S.; Cobb, J. E.; Lambert, M. H.; et al. Ligand Binding and Co-activator Assembly of the Peroxisome Proliferator-Activated Receptor- γ . *Nature* **1998**, *395*, 137–143.
- (5) Uppenberg, J.; Svensson, C.; Jaki, M.; Bertilsson, G.; Jendeborg, L.; et al. Crystal Structure of the Ligand Binding Domain of the Human Nuclear Receptor PPAR γ . *J. Biol. Chem.* **1998**, *273*, 31108–31112.
- (6) Xu, H. E.; Lambert, M. H.; Montana, V. G.; Plunket, G. M.; Moore, L. B.; et al. Structural Determinants of Ligand Binding Selectivity between the Peroxisome Proliferator-Activated Receptors. *PNAS* **2001**, *98*, 13919–13924.
- (7) Henke, B. R.; Blanchard, S. G.; Brackeen, M. F.; Brown, K. K.; Cobb, J. E.; et al. *N*-(2-Benzoylphenyl)-L-tyrosine PPAR γ Agonists. 1. Discovery of a Novel Series of Potent Antihyperglycemic and Antihyperlipidemic Agents. *J. Med. Chem.* **1998**, *41*, 5020–5036.
- (8) Collins, J. L.; Blanchard, S. G.; Boswell, G. E.; Charifson, P. S.; Cobb, J. E.; et al. *N*-(2-Benzoylphenyl)-L-tyrosine PPAR γ Agonists. 2. Structure–Activity Relationship and Optimization of the Phenyl Alkyl Ether Moiety. *J. Med. Chem.* **1998**, *41*, 5037–5054.
- (9) Cobb, J. E.; Blanchard, S. G.; Boswell, E. G.; Brown, K. K.; Charifson, P. S.; et al. *N*-(2-Benzoylphenyl)-L-tyrosine PPAR γ Agonists. 3. Relationship and Optimization of the *N*-Aryl Substituent. *J. Med. Chem.* **1998**, *41*, 5055–5069.
- (10) Henke, B. R.; Adkison, K. K.; Blanchard, S. G.; Leesnitzer, L. M.; A., R.; et al. Synthesis and Biological Activity of a Novel Series of Indole-Derived PPAR γ Agonists. *Bioorg. Med. Chem. Lett.* **1999**, *9*, 3329–3334.
- (11) Buckle, D. R.; Cantello, B. C. C.; Cawthorne, M. A.; Coyle, P. J.; Dean, D. K.; et al. Nonthiazolidinedione Antihyperglycemic Agents. 1: R-Heteroatom Substituted γ Phenylpropanoic Acids. *Bioorg. Med. Chem. Lett.* **1996**, *6*, 2121–2126.
- (12) Buckle, D. R.; Cantello, B. C. C.; Cawthorne, M. A.; Coyle, P. J.; Dean, D. K.; et al. Nonthiazolidinedione Antihyperglycemic Agents. 2: R-Carbon Substituted γ Phenylpropanoic Acids. *Bioorg. Med. Chem. Lett.* **1996**, *6*, 2127–2130.
- (13) Shinkai, H.; Onogi, S.; Tanaka, M.; Shibata, T.; Wao, M.; et al. Isoxazolidine-3,5-dione and Noncyclic 1,3-Dicarbonyl Compounds as Hypoglycemic Agents. *J. Med. Chem.* **1998**, *41*, 1927–1933.
- (14) Sauerberg, P.; Pettersson, I.; Jeppesen, L.; Bury, P. S.; Mogensen, J. P.; et al. Novel Tricyclic- α -alkyloxyphenylpropionic Acids: Dual PPAR α/γ Agonists with Hypolipidemic and Antidiabetic Activity. *J. Med. Chem.* **2002**, *45*, 789–804.
- (15) Kurogi, Y. Three-Dimensional Quantitative Structure–Activity Relationship (3D-QSAR) of Antidiabetic Thiazolidinediones. *Drug Des. Discovery* **1999**, *16*, 109–118.
- (16) Cramer, R. D.; Patterson, D. E.; Bunce, J. D. Comparative Molecular Field Analysis (CoMFA). 1. Effect of Shape on Binding of Steroids to Carrier Proteins. *J. Am. Chem. Soc.* **1988**, *110*, 5959–5967.
- (17) Klebe, G. Comparative Molecular Similarity Indices Analysis: CoMSIA. *Perspect. Drug Discovery Des.* **1998**, *12*, 87–104.
- (18) Klebe, G.; Abraham, U.; Mietzner, T. Molecular Similarity Indices in a Comparative Analysis (CoMSIA) of Drug Molecules To Correlate and Predict Their Biological Activity. *J. Med. Chem.* **1994**, *37*, 4130–4146.
- (19) Böhm, M.; Stürzebecher, J.; Klebe, G. Three-Dimensional Quantitative Structure–Activity Relationship Analyses Using Comparative Molecular Field Analysis and Comparative Molecular Similarity Indices Analysis To Elucidate Selectivity Differences of Inhibitors Binding to Trypsin, Thrombin, and Factor Xa. *J. Med. Chem.* **1999**, *42*, 458–477.
- (20) Ferguson, A. M.; Heritage, T.; Jonathon, P.; Pack, S. E.; Philips, L.; et al. EVA: A New Theoretically Based Molecular Descriptor for Use in QSAR/QSPR Analysis. *J. Comput.-Aided. Mol. Des.* **1997**, *11*, 143–152.
- (21) Turner, D. B.; Willett, P. Evaluation of the EVA Descriptor for QSAR Studies: 3. The Use of a Genetic Algorithm To Search for Models with Enhanced Predictive Properties (EVA_GA). *J. Comput.-Aided. Mol. Des.* **2000**, *14*, 1–21.

- (22) Turner, D. B.; Willett, P.; Ferguson, A. M.; Heritage, T. Evaluation of a Novel Infrared Range Vibration-Based Descriptor (EVA) for QSAR Studies. 1. General Application. *J. Comput.-Aided Mol. Des.* **1997**, *11*, 409–422.
- (23) Turner, D. B.; Willett, P.; Ferguson, A. M.; Heritage, T. W. Evaluation of a Novel Molecular Vibration-Based Descriptor (EVA) for QSAR Studies. 2. Model Validation Using a Benchmark Steroid Dataset. *J. Comput.-Aided Mol. Des.* **1999**, *13*, 271–296.
- (24) Makhija, M. T.; Kulkarni, V. M. Eigen Value Analysis of HIV-1 Integrase Inhibitors. *J. Chem. Inf. Comput. Sci.* **2001**, *41*, 1569–1577.
- (25) Ginn, C. M. R.; Turner, D. B.; Willett, P. Similarity Searching in Files of Three-Dimensional Chemical Structures: Evaluation of the EVA Descriptor and Combination of Ranking Using Data Fusion. *J. Chem. Inf. Comput. Sci.* **1997**, *37*, 23–37.
- (26) Heritage, T. W.; Ferguson, A. M.; Turner, D. B.; Willett, P. EVA: A Novel Theoretical Descriptor for QSAR Studies. *Perspect. Drug Discovery Des.* **1998**, 381–398.
- (27) SYBYL 6.81; Tripos Inc.: St. Louis, MO, 2001.
- (28) Parks, D. J.; Tomkinson, N. C. O.; Villeneuve, M. S.; Blanchard, S. G.; Willson, T. M. Differential Activity of Rosiglitazone Enantiomers at PPAR γ . *Bioorg. Med. Chem. Lett.* **1998**, *8*, 3657–3658.
- (29) Turner, D. B.; Willett, P. The EVA Spectral Descriptor. *Eur. J. Med. Chem.* **2000**, *35*, 367–375.
- (30) Bernstein, F. C.; Koetzle, T. F.; Williams, G. J.; Meyer, E. E., Jr.; Brice, M. D.; et al. The Protein Data Bank: A Computer-Based Archival File for Macromolecular Structures. *J. Mol. Biol.* **1977**, *112*, 535–542.
- (31) Gampe, R. T., Jr.; Montana, V. G.; Lambert, M. H.; Miller, A. B.; Bledsoe, R. K.; et al. Asymmetry in the PPAR γ /RXR α Crystal Structure Reveals the Molecular Basis of Heterodimerization Among Nuclear Receptors. *Mol. Cell* **2000**, *5*, 545–555.
- (32) Clark, M.; Cramer, R. D., III; Van Opdenbosh, N. Validation of the General Purpose Tripos 5.2 Force Field. *J. Comput. Chem.* **1998**, *10*, 982–1012.
- (33) Stewart, J. J. MOPAC: A Semiempirical Molecular Orbital Program. *J. Comput.-Aided Mol. Des.* **1990**, *4*, 1–105.
- (34) Liao, C. Z.; Xie, A. H.; Shi, L. M.; Zhou, J. J.; Lu, X. P. 3D QSAR Studies on Peroxisome Proliferator-Activated Receptor γ Agonists Using CoMFA and CoMSIA. *J. Mol. Mod.*, in press.
- (35) SYBYL Ligand-Based Design Manual, Version 6.81; Tripos: St. Louis, MO, 2001.

CI034109C